

# Guiding of Light with Pinholes

Makoto Morinaga

Institute for Laser Science, University of Electro-Communications  
Chofu, Tokyo, 182-8585 JAPAN

October 18, 2018

## Abstract

A new type of light waveguide using linearly aligned pinholes is presented. Results of basic experiments are compared with theoretical estimates calculated using continuous model. Since this waveguide utilizes no transparent material, it can be used to guide electromagnetic waves of wide wavelength ranges as well as other waves such as matter waves.

## 1 Introduction

Optical fibers are extremely useful as light waveguides and are widely used not only for classical communications[1] but also for quantum communications[2]. Their transmission loss can be especially low for some specific wavelength such as  $\lambda = 1.55\mu\text{m}$  where the absorption of silica glass is at minimum. Conversely, one needs a good transparent material to obtain a good transmissivity. In this paper, we propose a new type of waveguide composed of linearly aligned pinholes of same diameter (fig.1). Since no transparent material is required for

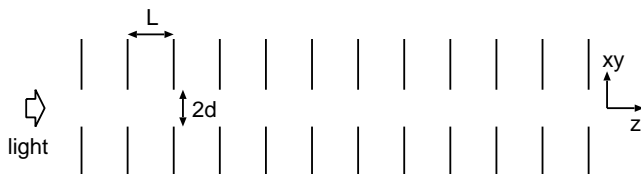


Figure 1: Construction of the pinhole waveguide. Pinholes of a diameter  $d$  are aligned on a straight line with spacing  $L$  between the pinholes.

its construction, it can be used to guide electromagnetic fields of wide frequency ranges, or waves of other kinds such as matter waves. Or it could also be used to guide and/or confine atoms with light guided by this pinhole waveguide because the space where light passes through is vacant. Such a structure is meaningless in geometrical optics since whether a ray transmits through this structure depends only on the geometrical arrangement of the ray and the first and the last pinholes, and pinholes in between play no role for the transmission. However, if we treat light as wave, as described in the appendix (see also [6]), transmission loss at each pinhole has a form  $\beta \left(\frac{\lambda L}{d^2}\right)^{\frac{3}{2}}$  where  $\lambda$  is the wavelength

of the light,  $L$  is the spacing between pinholes,  $d$  is the radius of the pinholes, and  $\beta$  is a constant that depends on the order of the transverse mode of the light (see fig.1). Thus the transmission loss per unit length is proportional to  $\sqrt{L}$  so that it can in principle be made arbitrary small by taking the spacing  $L$  between the pinholes smaller and smaller. In the following, we present basic experiments with pinhole waveguides and, in the appendix, we will outline a theoretical treatment of this waveguide using continuous model to analyze the experimental results.

## 2 Experiments with pinhole waveguides

The experimental setup is schematically shown in fig.2. A DPSS (Diode Pumped Solid State) laser module generates TEM<sub>00</sub> output of wavelength at both 1064nm and 532nm. 1064nm (532nm) wavelength is selected by inserting a VIS cut filter (IR cut filter). Part of the laser beam is reflected into a photo diode for power stabilization. When the laser beam enters the pinhole array, the beam size is considerably larger than the size of the pinhole and we can regard the incident wave as a plane wave. Each pinhole is mounted on a  $xy$ -translation stage which is fixed on a linear rail lying in  $z$ -direction. Up to 10 pinholes can be set on the rail with minimum spacing of 15mm (29mm to insert the image sensor or the power meter between the pinholes).

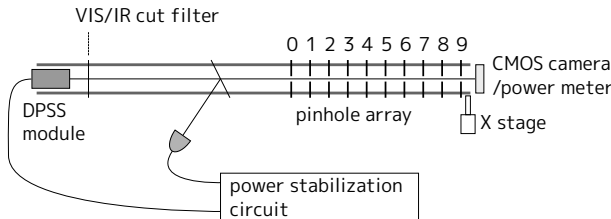


Figure 2: Light from a DPSS laser module propagates through pinholes and is detected by either a CMOS image sensor or a power meter at the end of the pinhole array which also can be inserted in between the pinholes.

### 2.1 Pinhole alignment

The alignment procedure of the pinholes on a straight line is as follows. The power meter is always set at the end of the pinhole array during this procedure and the light at 532nm wavelength is used. First we set no pinhole except the last pinhole (pinhole no.9 in fig.2) and maximize the power by adjusting the  $xy$ -position of this pinhole (the power is plotted as '0' in the horizontal axis of fig.3). Then we set the first pinhole (pinhole no.0 in fig.2) and maximize the power by adjusting the  $xy$ -position of this pinhole (plotted as '1' in the horizontal axis of fig.3). And then pinhole no.1 (plotted as '2'), pinhole no.2 (plotted as '3'), and so on. The spacing between the pinholes is  $L = 45\text{mm}$ . From fig.3 we see that the transmitted light power increases with increasing number of pinholes, which cannot be explained by geometrical optics.

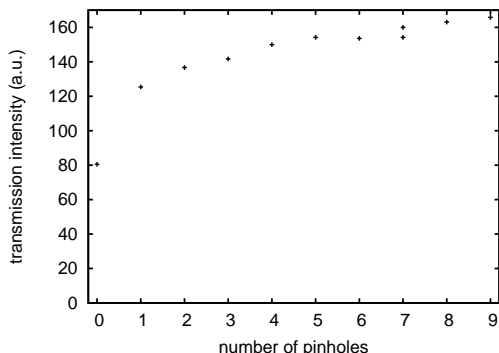


Figure 3: The power of the output of the pinhole array is plotted while inserting pinholes one by one (see text). Pinhole diameter:  $2d = 0.5\text{mm}$ . Light wavelength:  $\lambda = 532\text{nm}$ .

## 2.2 Propagation through the pinhole array

After aligning all the 10 pinholes light power after each pinhole is measured and compared with the theoretical curve calculated using the equation (17) in the appendix (fig.4). The theoretical curves are plotted with no fitting parameter except that initial power is normalized to 1 for both experiment and theory. The tendency that the experimental value is lower than the theoretical curve might be explained by the fact that the misalignment of the pinhole always decreases the power from that without misalignment. The initial square beam cut out from the incident plane wave contains high order transverse modes that attenuate fast compared with the lowest order mode leading to the initial rapid decay. After propagating through several pinholes, lowest order mode dominates then showing slower decay. In fig.5 beam images after the pinhole

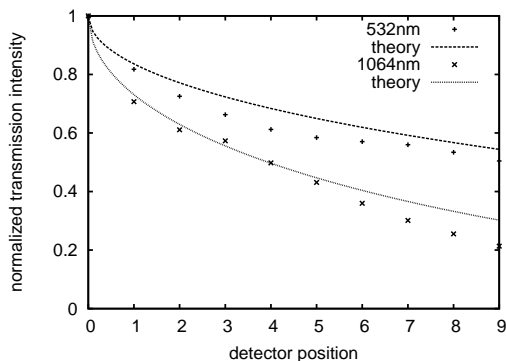


Figure 4: Light power after each pinhole is plotted. The power after the pinhole no.0 is normalized to 1. Pinhole spacing:  $L=45\text{mm}$ .  $2d = 0.5\text{mm}$ . Two lines are theoretical curves calculated using the continuous model.

no.0 and no.3 are shown ( $\lambda = 532\text{nm}$ ). The latter shows smooth profile with a peak intensity at the center which qualitatively confirms the explanation given

above (the distance of about 17mm from the pinhole to the image sensor makes fine structure in the left image due to diffraction).

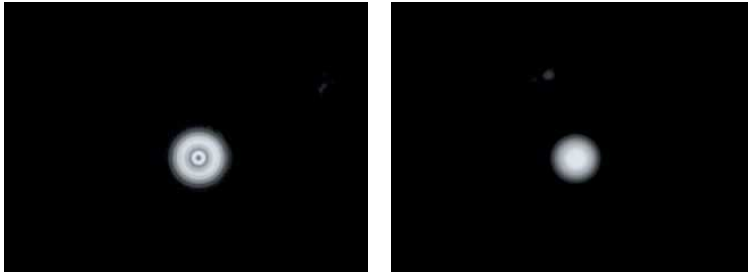


Figure 5: Beam image after pinhole no.0 (left) and pinhole no.3 (right).

### 2.3 Bending of light

The linear rail on which pinholes is sitting is fixed to the optical table at three points: at the left end, in the middle near the pinhole no.0, and at the right end. We remove the fixing screw at the right end and push this end to the transverse direction. Then the rail is bent elastically and the line on which pinholes lies is curved with a uniform curvature (fig.6). In fig.7 we plot the power of the

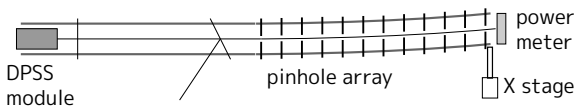


Figure 6: Schematics of the light bending experiment (see text).

output light versus the displacement of the last pinhole (pinhole no.9). The experimental value is compared with a theoretical curve assuming the geometrical optics. Certain amount of light is transmitted even with displacements larger than the diameter of the pinhole (0.5mm). Note also that the initial decrease seems to be quadratic in the displacement while geometrical optics predicts a linear response.

## 3 Conclusion and outlook

In this paper we presented basic experiments of light guiding with a pinhole array. The results roughly confirm the theoretical estimates carried out using continuous model. However further study is needed to understand the details of this new waveguide, such as how the thickness of the pinholes affects in the transmission.

### Acknowledgements

This work was partly supported by the AMADA FOUNDATION and the Photon Frontier Network Program (MEXT).

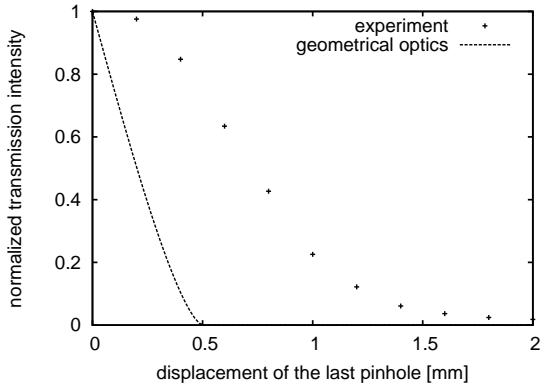


Figure 7: Power of the transmitted light is measured while bending the waveguide.  $2d = 0.5\text{mm}$ .  $\lambda = 532\text{nm}$ .  $L = 45\text{mm}$ . Dotted line is the theoretical curve following the geometrical optics.

## A Continuous model

Dealing directly with a discrete array of masks (pinholes, slits,...) for theoretical analysis is not an easy task. Instead, we introduce in this appendix a model in which the discrete set of masks is replaced with continuous medium of some absorbance that fills the closed region of the masks (see Fig. 8). This continuous model was first introduced for an array of half-planes to account the enhanced quantum reflection of matter waves from the ridged surfaces[3, 4]. The lowest order transverse mode function for the slit array and its loss parameter are also calculated already[5]. Here we will determine all the transverse mode functions and their propagation parameter for the case of the slit array and the pinhole array. The light field is treated as a scalar field (scalar theory). The wave

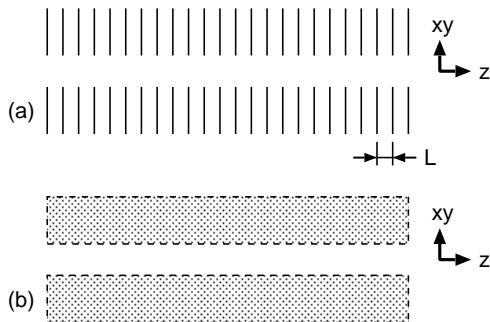


Figure 8: (a) Array of masks separated by  $L$ . (b) The mask array is replaced with continuous absorbing medium.

equation for this model is given by

$$-k_0^2 \psi(x, y, z) = \{1 - i\epsilon \theta(x, y)\} \nabla^2 \psi(x, y, z)$$

where  $k_0$  is the wavenumber of light,  $\theta(x, y)$  is a step function that takes value 1 (0) in the closed (open) region of masks, and  $\epsilon$  is a positive constant related to the absorptance of the medium. As we shall see below  $\epsilon \ll 1$  for our system under consideration. First we consider a plane wave propagating through the area filled uniformly with such absorbing medium. Taking  $z$ -axis as the direction of propagation, the wave equation is written as

$$-k_0^2 \psi(z) = (1 - i\epsilon) \psi''(z).$$

Its solution is given by

$$\psi(z) = e^{ik_z z}$$

with  $k_0^2 = (1 - i\epsilon)k_z^2 \approx \left\{ \left(1 + \frac{i}{2}\epsilon\right)^{-1} k_z \right\}^2$  so that  $k_z = \left(1 + \frac{i}{2}\epsilon\right) k_0$  and  $|\psi(z)|^2 = e^{-\zeta_0 z}$  with the intensity absorptance  $\zeta_0 = \epsilon k_0$ . Given that this absorbing medium imitates a stack of opaque masks separated by a distance  $L$ , we expect that  $\zeta_0 \sim \frac{1}{L}$  so that  $\epsilon \sim \frac{1}{k_0 L}$ . Thus we shall write  $\epsilon = \frac{\xi}{k_0 L}$  with a positive parameter  $\xi$  of order of 1. We consider the parameter region where the separation of masks  $L$  is much larger than the wavelength, so that  $\epsilon \ll 1$ . The continuous model itself cannot determine the value of  $\xi$  (or  $\epsilon$ ). By comparing the attenuation of a wave propagating in a slit waveguide calculated using continuous model with that calculated with direct method[6] it is shown that

$$\xi = \frac{9}{2}\pi. \quad (1)$$

## A.1 Slit array

Consider an array of slits of opening width  $2d$  (open for  $|x| < d$ ). The wave equation is written as

$$-k_0^2 \psi(x, z) = \{1 - i\epsilon \theta(x^2 - d^2)\} (\partial_x^2 + \partial_z^2) \psi(x, z)$$

where  $\theta$  is the conventional step function defined as

$$\theta(s) \equiv \begin{cases} 0 & (s < 0) \\ 1 & (s \geq 0) \end{cases}.$$

Because of the translational symmetry in  $z$ -axis direction, we can assume the form of the solution as  $\psi(x, z) = \varphi(x) e^{ik_z z}$  (a general solution is the sum of such solutions). Below we also assume that the wave propagates nearly in  $z$  direction so that  $k_z \approx k_0$ .

**Region A (inside the opening of slits)  $|x| \leq d$**  The wave equation for the transverse wavefunction  $\varphi(x)$  here is

$$-(k_0^2 - k_z^2) \varphi(x) = \varphi''(x)$$

with a solution

$$\varphi(x) = \text{cs}(k_A x),$$

where  $\text{cs}$  is defined as

$$\text{cs}(u) = \begin{cases} \cos u & (\text{even parity}) \\ \sin u & (\text{odd parity}) \end{cases}, \quad (2)$$

and  $k_A$  satisfies  $k_0^2 = k_A^2 + k_z^2$ . We are considering the situation in which the wave is nearly confined in the opening region  $|x| \leq d$  and hence  $\varphi(\pm d) \approx 0$ , so that  $k_A d \approx \frac{n+1}{2}\pi$  ( $n = 0, 1, 2, \dots$ ) provided that we use  $\cos$  ( $\sin$ ) in (2) for even (odd)  $n$ . Defining  $k_n \equiv \frac{n+1}{2d}\pi$  and write  $k_A = k_n + \beta + i\gamma$  with real numbers  $\beta$  and  $\gamma$ , then  $|\beta d| \ll 1$  and  $|\gamma d| \ll 1$ .

$$\begin{aligned}\varphi(\pm d) &= \text{cs}(\pm k_A d) \approx \pm(\beta + i\gamma)d \text{cs}'(\pm k_n d) \\ \varphi'(\pm d) &= k_A \text{cs}'(\pm k_A d) \approx k_n \text{cs}'(\pm k_n d) \\ \frac{\varphi'}{\varphi} \Big|_{x=\pm d} &\approx \pm \frac{k_n}{(\beta + i\gamma)d}\end{aligned}\quad (3)$$

**Region B (outside the opening of slits):**  $|x| \geq d$  Here the wave equation is

$$-\{k_0^2 - (1 - i\epsilon)k_z^2\}\varphi(x) = (1 - i\epsilon)\varphi''(x)$$

so that the solution is, taking into account that it should not diverge when  $x \rightarrow \pm\infty$ ,

$$\varphi(x) \propto e^{ik_B|x|} \quad (4)$$

where  $k_B$  satisfies  $k_0^2 = (1 - i\epsilon)(k_B^2 + k_z^2)$  and  $\text{Im } k_B > 0$  (the proportionality factor in (4) has opposite sign for  $x \geq d$  and  $x \leq -d$  for the odd parity solution). Thus

$$\frac{\varphi'}{\varphi} \Big|_{x=\pm d} = \pm ik_B \quad (5)$$

**Boundary condition at  $x = \pm d$**  By requiring  $\varphi(x)$  and  $\varphi'(x)$  is continuous at  $x = \pm d$ , from (3) and (5) we find

$$ik_B = \frac{k_n}{(\beta + i\gamma)d}. \quad (6)$$

By noting  $k_B^2 - k_A^2 = \frac{i\epsilon}{1-i\epsilon}k_0^2$  and

$$|k_B| = \frac{|k_n|}{|\beta + i\gamma|d} \gg |k_n| \approx |k_A|,$$

we see

$$k_B^2 \approx i\epsilon k_0^2 \quad (7)$$

so that

$$k_B = \frac{1+i}{\sqrt{2}}\sqrt{\epsilon}k_0. \quad (8)$$

Using (6)

$$\beta + i\gamma = \frac{k_n}{ik_B d} = -\frac{1+i}{\sqrt{2}}\frac{k_n}{\sqrt{\epsilon}k_0 d}$$

and we obtain

$$k_A = k_n + \beta + i\gamma = \left(1 - \frac{1+i}{\sqrt{2\epsilon}k_0 d}\right)k_n. \quad (9)$$

From the assumption that  $|\beta d| \ll 1$  and  $|\gamma d| \ll 1$  we see  $\sqrt{\epsilon}k_0 d \gg 1$ , i.e.

$$\frac{L}{k_0 d^2} = \frac{1}{2\pi} \frac{\lambda L}{d^2} \ll 1. \quad (10)$$

Finally  $k_z$  is derived as

$$k_z = \sqrt{k_0^2 - k_A^2} \approx k_0 - \frac{1}{2} \frac{k_A^2}{k_0} \approx k_0 - \frac{k_n^2}{2k_0} + \frac{k_n^2}{\sqrt{2\epsilon}k_0^2 d} i \quad (11)$$

From this we calculate the light attenuation along the waveguide

$$|e^{ik_z z}|^2 = e^{-\zeta z}$$

where the attenuation coefficient  $\zeta = 2\text{Im} k_z$  is calculated as

$$\zeta = \frac{\sqrt{2}k_n^2}{\sqrt{\epsilon}k_0^2 d} = (n+1)^2 \frac{\sqrt{2}\pi^2}{4\sqrt{\epsilon}k_0^2 d^3} = (n+1)^2 \frac{\sqrt{2}L\pi^2}{4\sqrt{\xi}k_0^3 d^3}$$

using  $\epsilon = \frac{\xi}{k_0 L}$ . The attenuation per length  $L$  (i.e. per one slit)  $\zeta L$  can be written as a function of a single dimensionless parameter  $\frac{\lambda L}{d^2}$ :

$$\zeta L = (n+1)^2 \frac{\sqrt{2}\pi^2}{4\sqrt{\xi}} \left( \frac{L}{k_0 d^2} \right)^{\frac{3}{2}} = (n+1)^2 \frac{\sqrt{\pi}}{8\sqrt{\xi}} \left( \frac{\lambda L}{d^2} \right)^{\frac{3}{2}}$$

## A.2 Pinhole array

In the case of an array of pinholes of diameter  $d$ , using cylindrical coordinate  $(r, \phi, z)$ , the wave equation is written as

$$-k_0^2 \psi(r, \phi, z) = \{1 - i\epsilon \theta(r^2 - d^2)\} \left( \partial_r^2 + \frac{1}{r} \partial_r + \frac{1}{r^2} \partial_\phi^2 + \partial_z^2 \right) \psi(r, \phi, z).$$

In the same way as in the case of slit array, we shall derive a solution of the form  $\psi(r, \phi, z) = \varphi(r, \phi) e^{ik_z z}$  with  $k_z \approx k_0$ .

**Region A (inside the opening of pinholes):**  $|r| \leq d$  The wave equation

$$-(k_0^2 - k_z^2) \varphi(r, \phi) = \left( \partial_r^2 + \frac{1}{r} \partial_r + \frac{1}{r^2} \partial_\phi^2 \right) \varphi(r, \phi)$$

is solved using the Bessel functions of the 1st kind  $J_m$  ( $m = 0, \pm 1, \pm 2, \dots$ ):

$$\varphi(r, \phi) = J_m(k_A r) e^{im\phi}$$

where  $k_A$  satisfies  $k_0^2 = k_A^2 + k_z^2$ . Again we postulate  $\varphi(d, \phi) \approx 0$  which leads to  $k_A d \approx \rho_n^{(m)}$  ( $n = 0, 1, 2, \dots$ ). Here  $\rho_0^{(m)}, \rho_1^{(m)}, \rho_2^{(m)}, \dots$  are positive zeros of  $J_m(\rho)$  sorted in ascending order. We define  $k_n^{(m)} \equiv \frac{\rho_n^{(m)}}{d}$  and write  $k_A = k_n^{(m)} + \beta + i\gamma$  using real numbers  $\beta$  and  $\gamma$  with  $|\beta d| \ll 1$  and  $|\gamma d| \ll 1$ .

$$\varphi(d, \phi) = J_m(k_A d) e^{im\phi} \approx (\beta + i\gamma) d J'_m(k_n d) e^{im\phi}$$

$$\partial_r \varphi|_{(d, \phi)} = k_A J'_m(k_A d) e^{im\phi} \approx k_n^{(m)} J'_m(k_n^{(m)} d) e^{im\phi}$$

$$\frac{\partial_r \varphi}{\varphi} \Big|_{(d, \phi)} \approx \frac{k_n^{(m)}}{(\beta + i\gamma) d} \quad (12)$$



**Region B (outside the opening of pinholes):**  $|r| \geq d$  The wave equation is written as

$$-\{k_0^2 - (1 - i\epsilon)k_z^2\}\varphi(r, \phi) = (1 - i\epsilon) \left( \partial_r^2 + \frac{1}{r}\partial_r + \frac{1}{r^2}\partial_\phi^2 \right) \varphi(r, \phi)$$

so that the solution is given by

$$\varphi \propto H_m^{(1)}(k_B r) e^{im\phi}$$

if we take into account its behavior when  $r \rightarrow \infty$  ( $H_m^{(1)}$  are the Hankel functions of the 1st kind). Here  $k_B$  satisfies  $k_0^2 = (1 - i\epsilon)(k_B^2 + k_z^2)$ . Noting that  $k_B^2 d^2 - k_A^2 d^2 = \frac{i\epsilon}{1-i\epsilon} k_0^2 d^2$  and that the absolute value of the right-hand side is much larger than 1 (see (10)) whereas  $k_A d$  in the left-hand side is of order of 1 so that we can neglect this term and (7) and (8) holds as in the case of slit array. From these we see that  $|k_B d| \gg 1$  and  $\arg k_B d \approx \frac{\pi}{4}$  (so that  $-\pi < \arg k_B d < 2\pi$ ), so that we can use the following asymptotic form of  $H_n^{(1)}$  for  $\rho = k_B d$  (see [7]):

$$\begin{aligned} H_m^{(1)}(\rho) &\approx \sqrt{\frac{2}{\pi\rho}} \exp\left(i\left[\rho - \frac{2m+1}{4}\pi\right]\right) \\ H_m^{(1)\prime}(\rho) &\approx i\sqrt{\frac{2}{\pi\rho}} \exp\left(i\left[\rho - \frac{2m+1}{4}\pi\right]\right) \end{aligned}$$

so that finally we obtain

$$\left. \frac{\partial_r \varphi}{\varphi} \right|_{(d, \phi)} = ik_B. \quad (13)$$

**Boundary condition at  $r = d$**  Continuity of  $\varphi(r, \phi)$  and  $\partial_r \varphi(r, \phi)$  at  $r = d$  yields, from (12) and (13),

$$ik_B = \frac{k_n^{(m)}}{(\beta + i\gamma)d}. \quad (14)$$

(14) has the same form as (5) with  $k_n$  replaced by  $k_n^{(m)}$ , so that similar to the case of slit array, we obtain

$$\begin{aligned} k_A &= k_n^{(m)} + \beta + i\gamma = \left(1 - \frac{1+i}{\sqrt{2\epsilon}k_0 d}\right) k_n^{(m)} \\ k_z &= \sqrt{k_0^2 - k_A^2} \approx k_0 - \frac{k_n^{(m)2}}{2k_0} + \frac{k_n^{(m)2}}{\sqrt{2\epsilon}k_0^2 d} i \end{aligned}$$

From this the attenuation of light along the waveguide

$$|e^{ik_z z}|^2 = e^{-\zeta z}$$

is calculated giving the attenuation coefficient  $\zeta = 2\text{Im} k_z$  as

$$\zeta = \frac{\sqrt{2}k_n^{(m)2}}{\sqrt{\epsilon}k_0^2 d} = \frac{\sqrt{2}\rho_n^{(m)2}}{\sqrt{\epsilon}k_0^2 d^3} = \frac{\sqrt{2L}\rho_n^{(m)2}}{\sqrt{\xi}k_0^3 d^3} \quad (15)$$

and the attenuation per length  $L$  (i.e. per one pinhole)  $\zeta L$  is given by

$$\zeta L = \frac{\sqrt{2}\rho_n^{(m)2}}{\sqrt{\xi}} \left(\frac{L}{k_0 d^2}\right)^{\frac{3}{2}} = \frac{\rho_n^{(m)2}}{2\sqrt{\xi}\pi^3} \left(\frac{\lambda L}{d^2}\right)^{\frac{3}{2}}.$$

### A.3 Attenuation of a multi-transverse-mode light

In the previous section we estimated the attenuation of a single transverse mode wave. Each transverse mode is specified by a pair  $(m, n)$  of an integer  $m$  and a non-negative integer  $n$ , and if the wave is confined tightly enough in the pinhole waveguide, the transverse mode functions are given by

$$\varphi_{mn}(r, \phi) = \begin{cases} \alpha_{mn} J_m(k_n^{(m)} r) e^{im\phi} & (r \leq d) \\ 0 & (r > d) \end{cases}$$

( $\alpha_{mn}$  are the normalization factors). Note that these are the Bessel beam transverse mode functions clipped at one of their nodes in the radial direction. The orthonormal condition is written as

$$\delta_{mm'} \delta_{nn'} = \langle \varphi_{mn}, \varphi_{m'n'} \rangle = \int_0^\infty r dr \int_0^{2\pi} d\phi \varphi_{mn}^*(r, \phi) \varphi_{m'n'}(r, \phi).$$

In this section we consider, as an example, the case where a plane wave  $\psi_p = \frac{1}{\sqrt{\pi d^2}} e^{ik_0 z}$  is incident into the waveguide, and calculate how the wave attenuates while it propagates along the waveguide. The incident wavefront is cut out at the input end of the waveguide (we take the input end as  $z = 0$ ) giving the transverse wave function as

$$\varphi_p(r, \phi) = \frac{1}{\sqrt{\pi d^2}} \theta(d^2 - r^2)$$

and such wavefront is, from the symmetry consideration, expanded with only  $m = 0$  modes:

$$\varphi_p = \sum_{n=0}^{\infty} \beta_n \varphi_{0n} \quad (16)$$

By integrating the square of absolute value of both sides of the above equation in  $(r, \phi)$  plane, we see that  $\sum_{n=0}^{\infty} |\beta_n|^2 = 1$ . The power attenuation is given by

$$P(z) = \sum_{n=0}^{\infty} |\beta_n|^2 \exp(-\zeta_n^{(0)} z). \quad (17)$$

Here  $\zeta_n^{(m)}$  is  $\zeta$  given in (15). By taking inner product of both sides of (16) with  $\varphi_{0n}$ ,

$$\beta_n = \langle \varphi_{0n}, \varphi_p \rangle = 2\pi \alpha_{0n}^* \frac{1}{\sqrt{\pi d^2}} \int_0^d r dr J_0(k_n^{(0)} r) = \frac{2\sqrt{\pi} \alpha_{0n}^* J_1(\rho_n^{(0)})}{k_n^{(0)}} = \frac{2}{\rho_n^{(0)}}$$

Here we used  $\frac{d}{d\rho}(\rho J_1(\rho)) = \rho J_0(\rho)$  and the value of  $\alpha_{0n}$  derived in the next subsection (18).

### A.4 Normalization factors $\alpha_{0n}$

From the normalization conditions of  $\varphi_{0n}$  we find

$$1 = \langle \varphi_{0n}, \varphi_{0n} \rangle = 2\pi |\alpha_{0n}|^2 \int_0^d r dr J_0^2(k_n^{(m)} r) = \pi |\alpha_{0n}|^2 d^2 J_1^2(\rho_n^{(0)}).$$

Here we used the formula

$$\frac{d}{d\rho} \left\{ \rho^2 \frac{J_0(\rho)^2 + J_1(\rho)^2}{2} \right\} = 2\rho J_0(\rho)^2$$

and  $J_0(\rho_n^{(0)}) = 0$ .  $\alpha_{0n}$  are determined as, besides the phase factor,

$$\alpha_{0n} = \frac{1}{\sqrt{\pi} d J_1(\rho_n^{(0)})}. \quad (18)$$

## References

- [1] G. P. Agrawal, Fiber-Optic Communication Systems, 4th ed., John Wiley & Sons (2010)
- [2] N. Gisin, S. Iblisdir, W. Tittel, and H. Zbinden, Quantum Communications with Optical Fibers, in: A. V. Sergienko (Eds.), Quantum Communications and Cryptography, Taylor & Francis (2006) Chapter 2
- [3] D. Kouznetsov and H. Oberst, Reflection of waves from a ridged surface and the Zeno effect, Opt. Rev. **12** (2005) 363
- [4] D. Kouznetsov and H. Oberst, Scattering of waves at ridged mirrors, Phys. Rev. A **72** (2005) 013617
- [5] D. Kouznetsov and M. Morinaga, Guiding of waves between absorbing walls, J. Mod. Phys. **3** (2012) 553
- [6] M. Morinaga, *in preparation*.
- [7] NIST Digital Library of Mathematical Functions §10.17  
<http://dlmf.nist.gov/10.17>